Recruitment of resting vesicles into recycling pools supports NMDA receptor-dependent synaptic potentiation in cultured hippocampal neurons

Arjuna Ratnayaka[1], Vincenzo Marra[1], Daniel Bush[1], Jemima J Burden[2], Tiago Branco[3,4] and Kevin Staras[1]

[1]*School of Life Sciences, University of Sussex, Brighton BN1 9QG, UK*
[2]*Medical Research Council Laboratory for Molecular Cell Biology and Cell Biology Unit, University College London, London WC1E 6BT, UK*
[3]*Wolfson Institute for Biomedical Research and* [4]*Department of Neuroscience, Physiology and Pharmacology, University College London, London WC1E 6BT, UK*

The Journal of Physiology

Key points

- Presynaptic terminals in hippocampal neurons are characterized by two functionally defined vesicle populations: a recycling pool, which supports activity-evoked neurotransmission, and a resting pool.
- Between individual synapses, the relative proportions of these two pools are highly variable, suggesting that this parameter might be specifically regulated to support changes in synaptic efficacy.
- Using fluorescence imaging and correlative ultrastructural approaches we show here that a form of synaptic potentiation dependent on *N*-methyl-D-aspartic acid (NMDA) receptor activity can lead to a rapid and sustained expansion of the recycling fraction at the expense of the resting pool.
- This recruitment of vesicles depends on nitric oxide signalling and calcineurin activity, and is accompanied by an increase in synaptic release probability.
- We suggest that vesicle exchange between these pools provides a rapid mechanism to support adjustments in synaptic strength associated with a form of Hebbian plasticity.

Abstract Most presynaptic terminals in the central nervous system are characterized by two functionally distinct vesicle populations: a recycling pool, which supports action potential-driven neurotransmitter release via vesicle exocytosis, and a resting pool. The relative proportions of these two pools are highly variable between individual synapses, prompting speculation on their specific relationship, and on the possible functions of the resting pool. Using fluorescence imaging of FM-styryl dyes and synaptophysinI-pHluorin (sypHy) as well as correlative electron microscopy approaches, we show here that Hebbian plasticity-dependent changes in synaptic strength in rat hippocampal neurons can increase the recycling pool fraction at the expense of the resting pool in individual synaptic terminals. This recruitment process depends on NMDA-receptor activation, nitric oxide signalling and calcineurin and is accompanied by an increase in the probability of neurotransmitter release at individual terminals. Blockade of actin-mediated intersynaptic vesicle exchange does not prevent recycling pool expansion demonstrating that vesicle recruitment is intrasynaptic. We propose that the conversion of resting pool vesicles to the functionally recycling pool provides a rapid mechanism to implement long-lasting changes in presynaptic efficacy.

Introduction

Central presynaptic terminals are characterized by a cluster of synaptic vesicles that support neurotransmitter release and information transfer between neurons (Pechstein & Shupliakov, 2010; Sudhof, 2004; Rizzoli & Betz, 2005). In hippocampal synapses, this population of vesicles can be functionally sub-classified into a recycling fraction, which readily undergoes vesicle exocytosis and turnover, and a residual resting pool. While the relationship between recycling pool properties and synaptic performance has been extensively characterized (Fernandez-Alfonso & Ryan, 2006; Schweizer & Ryan, 2006), a definitive role for resting pool vesicles remains unclear. In recent years, evidence has emerged to suggest that some resting vesicles may support spontaneous release (Sara *et al.* 2005; Fredj & Burrone, 2009) but this remains controversial (Groemer & Klingauf, 2007; Hua *et al.* 2010; Wilhelm *et al.* 2010).

The magnitude, organization and release properties of presynaptic vesicle pools are recognized targets for modulation associated with forms of plasticity (Malgaroli *et al.* 1995; Ryan *et al.* 1996; Ma *et al.* 1999; Antonova *et al.* 2001; Murthy *et al.* 2001; Zakharenko *et al.* 2001; Micheva & Smith, 2005; Thiagarajan *et al.* 2005; Wang *et al.* 2005; Ninan *et al.* 2006; Tyler *et al.* 2006; Antonova *et al.* 2009; Ostroff *et al.* 2011). Since recycling pool size is known to correlate tightly with synaptic release probability (Murthy *et al.* 1997), one attractive hypothesis is that recruitment of resting vesicles to recycling pools could be used as a fast mechanism to support plasticity-dependent changes in synaptic efficacy. Indirect evidence in support of this idea comes from findings by a number of groups showing that the size of the recycling pool, expressed as a fraction of the total pool, is highly variable across synapses (Harata *et al.* 2001*b*; Li *et al.* 2005; Micheva & Smith, 2005; Fernandez-Alfonso & Ryan, 2008; Fredj & Burrone, 2009; Branco *et al.* 2010; Kim & Ryan, 2010; Welzel *et al.* 2011) suggesting that this parameter may be under specific regulation. Moreover, recent work has characterized a molecular control mechanism for the setting of resting pool size which has been implicated in a form of homeostatic scaling (Kim & Ryan, 2010).

Here we examine recycling pool fractions in synapses that have undergone activity-dependent plasticity requiring NMDA-receptor (NMDAR) activation. Using chemical and genetically encoded optical probes which report recycling pool sizes, we demonstrate that synaptic potentiation is associated with an increase in the recycling pool fraction at the expense of the resting pool, and a rise in synaptic release probability. Correlative light and electron microscopy approaches provide a direct ultrastructural view of synaptic pool reorganization. Pharmacological experiments show that potentiation is dependent on nitric oxide (NO) signalling and calcineurin activity but not actin polymerization, suggesting that recruitment of vesicles from outside the terminal is not required to support the expansion of the recycling pool. Our findings show that recruitment of resting vesicles into functional pools is an important mechanism to achieve activity-dependent plastic changes at hippocampal presynaptic terminals, with immediate functional impact.

Methods

Ethical information

Experiments were performed in accordance with the UK Animals (Scientific Procedures) Act 1986. P0 rat pups were humanely killed by cervical dislocation and decapitation under Schedule 1.

Cell culture and transfections

Dissociated hippocampal cultures were prepared from P0 rats as described previously (Darcy *et al.* 2006*a*) and used for experiments at 11–18 days *in vitro*. Neurons were transfected at days *in vitro* 7–9, using a calcium phosphate protocol (Promega Corp., Madison, WI, USA). Unless otherwise stated, all experiments were performed in external bath solution with the following composition: 137 mM NaCl, 5 mM KCl, 2.5 mM $CaCl_2$, 1 mM $MgCl_2$, 10 mM D-glucose, 5 mM Hepes, 20 μM 6-cyano-7-nitroquinoxaline-2,3-dione (CNQX, Tocris Bioscience, Bristol, UK), 50 μM D(−)-2-amino-5-phosphonovaleric acid (AP5, Tocris) at $23 \pm 1°C$

Labelling, imaging and fluorescence analysis

FM-dye labelling of recycling synaptic vesicles was achieved using field stimulation (600 APs, 10 Hz) (Ryan & Smith, 1995) in the presence of the dye (FM1-43 or FM4-64, 10 μM, Molecular Probes). After loading, cells were washed with fresh external bath solution for 10 min to remove surface dye. For plasticity experiments, we investigated changes in recycling pool sizes by using two rounds of FM-dye loading, the first with FM4-64 and the second, 20 min after the plasticity protocol, with FM1-43. The analysed images were generated from maximum intensity projections of image stacks (see below). This dual dye method allowed us to monitor recycling pools independently for each load without concerns about residual fluorescence from the first dye exposure contaminating the signal in the second load. Validation of this method is provided in Fig. 2. We also used an alternative method for quantifying recycling vesicle pools: activation of synaptophysinI-pHluorin (sypHy)-expressing neurons (Granseth *et al.* 2006) in the presence of bafilomycin (1 μM, Calbiochem), which traps

vesicles in an alkaline state (Sankaranarayanan & Ryan, 2001). The recycling pool was revealed by stimulation at 20 Hz (1200 APs). In our experiments we found that the signal typically plateaued after 500 APs, suggesting that the recycling pool was fully turned over at this point. A relative measure of the recycling pool fraction was achieved by measuring the total pool after addition of 50 mM NH_4Cl (replacing 50 mM NaCl in the saline) (Fernandez-Alfonso & Ryan, 2008). For each step in this experiment (bafilomycin pre-stim, bafilomycin+1200 APs, NH_4Cl) the analysed image was generated from a maximum intensity projection image from an image stack (see below). For all experiments, plasticity was induced by stimulating cultures with 6×100 APs at 20 Hz (every 5 s) in modified extracellular solution (3 mM $CaCl_2$–0.5 mM $MgCl_2$ or 3.5 mM $CaCl_2$–0 mM $MgCl_2$) without AP5. Control experiments were carried out in the same external solutions but with combinations of blockers (AP5+CNQX, AP5 only, CNQX only). In some experiments we imaged FM1-43 in neurons expressing the genetically encoded construct synaptophysinI-mCherry (sypI-mCherry); in this way, the recycling and total vesicle pools could be visualized together in the same synaptic terminals. Epifluorescence images were acquired using an Olympus BX61WI microscope with a $60\times$ 1.0 NA dipping objective. Excitation and emission filter sets for fluorescent probes were as follows: FM1-43 and sypHy, 470/22, 520/35; FM4-64, 470/22, 624/40; sypI-mCherry 556/22, 624/40. For all quantitative experiments, we collected images using z-stacks ($13 \times 0.75\,\mu$m planes for FM-dye experiments, $17 \times 0.5\,\mu$m planes for sypHy experiments) allowing us to gather representative fluorescence readouts from all synapses across different focal planes. Analysed images were based on maximum intensity projections.

Image analysis and puncta identification

Image analysis was performed using ImageJ (http://rsb. info.nih.gov/ij/) and MATLAB (The Mathworks, Inc., Natick, MA, USA). Quantification of fluorescence was carried out using ImageJ (NIH) on raw unfiltered images or after filtering (1×1 median filter) applied to the whole image. Curve fitting and statistical analyses were performed with Prism (GraphPad Software Inc., La Jolla, CA, USA). Student's *t* test or Mann–Whitney's test was used, as appropriate, to perform two-group comparisons. Comparisons between multiple conditions used one-way ANOVA followed by *post hoc* comparisons for each condition using Tukey's test. For analysis of FM-dye puncta in pre–post plasticity images, custom-written MATLAB software was used. Background subtraction was performed on each aligned image by identifying the lowest non-zero point of the fluorescence histogram and subtracting this background fluorescence signal from the

intensity values for each pixel, resetting any negative values to zero. The raw image was then converted to a series of binary matrices by thresholding at multiple relative fluorescence values, from 5% to 95% of the maximum intensity in steps of 10%. Putative synaptic puncta were subsequently identified as interconnected regions with an area $<4.5\,\mu$m^2 that were present in a summed amalgamation of the binary matrices for each relative intensity threshold. Pairs of putative synaptic puncta that were unequivocally present in both images (i.e. pre- and post-tetanus) could then be selected, and statistics pertaining to the area, integrated and mean fluorescence of each were extracted and compared.

Measurement of p_r

Release probability estimates were based on FM-dye destaining experiments (Branco *et al.* 2008) (1 Hz stimulation over 10 min) using maximum intensity projections of z-stacks ($5 \times 0.75\,\mu$m planes). To negate potential concerns about analysing non-functional synapses, we applied a single exponential fit to all dye-loss profiles and restricted analysis to synapses with a destaining time constant (τ) of <8 min. The fluorescence of each FM-dye punctum was quantified using a custom-written algorithm in MATLAB and the time constant of the fit was used to calculate the mean fraction of recycling pool vesicles released per action potential (Branco *et al.* 2008). To convert this to a p_r estimate we used a mean recycling pool size value of 127 vesicles for control (Ryan *et al.* 1997; Branco *et al.* 2008) and 159 for potentiated synapses, based on our electron microscopy (EM) measurements. Values of p_r above 1 were excluded from the analysis.

Pharmacology

To test the effect of inhibiting calcineurin on potentiation, cells were incubated in the blocker FK506 (1 μM, Tocris) (Kumashiro *et al.* 2005) during the tetanus between successive rounds of FM4-64 and FM1-43 dye labelling. Analysis was carried out on maximum intensity projection images from a z-stack ($13 \times 0.75\,\mu$m planes). Effects of N^ω-nitro-L-arginine (L-NA, 100 μM, Sigma) (Wang *et al.* 2005) or jasplakinolide (1 μM, Calbiochem) (Darcy *et al.* 2006a) were investigated by preincubation during the tetanus period followed by measurement of recycling fractions using the alkaline trapping method in sypHy-expressing neurons. The tetanic stimulation was carried out in 3 mM $CaCl_2$, 0.5 mM $MgCl_2$, as above. Analysis was performed on maximum intensity projection images from a z-stack ($17 \times 0.50\,\mu$m planes). For all treatments, FM-dye destaining and/or stimulation-evoked

sypHy-dequenching demonstrated that synaptic vesicle recycling was not compromised.

Photoconversion and electron microscopy

For ultrastructural investigation of recycling vesicle pool fractions, experimental and control cultures subjected to the tetanic stimulation protocol were labelled with $10\,\mu\text{M}$ FM1-43FX, a fixable form of FM1-43 (Molecular Probes). Photoconversion procedures were the same as outlined previously (Staras *et al.* 2010). Briefly, FM1-43FX labelled cultures were fixed (2% paraformaldehyde–2% glutaraldehyde, 15 min) and photoconverted following a 10 min pre-incubation in diaminobenzidine (DAB, $1\,\text{mg ml}^{-1}$, Kem-En-Tec Diagnostics, Taastrup, Denmark). Target regions from fluorescence experiments were re-identified and brightfield images acquired using an Olympus BX51WI upright microscope. Photoconversion involved illumination of the sample for 11 min with 470 nm light from a LED source. Neurons were rinsed in phosphate-buffered saline (PBS), osmicated, stained with tannic acid, dehydrated stepwise in ethanol and embedded in EPON (TAAB) as previously described (Darcy *et al.* 2006*b*). Serial sections of embedded neurons were placed on Formvar coated slot grids. Samples were viewed using a Hitachi 7100 electron microscope and images were acquired with a 2048×2048 cooled CCD camera (Gatan Inc., Pleasanton, CA, USA). To provide an unbiased sampling of synapses we identified puncta using our custom written software and generated fluorescence intensity distribution curves for experimental and control synapses. All puncta in the top 40% of the distribution were then targeted in EM by generating a fluorescence overlay on electron micrographs. Of these synapses we could unequivocally correlate a subset in our EM samples (tetanus: 28 synapses, mean section number: 4.39; tetanus + block: 37 synapses, mean section number: 4.13). For calculating vesicle fractions the quantification of vesicles as photoconverted (PC^+) or non-photoconverted (PC^-) was carried out based on methods described previously (Darcy *et al.* 2006*a*). We assumed an equal mixing of recycling vesicles within the total vesicle pool consistent with our previous analysis (Darcy *et al.* 2006*a*) and that of others (Harata *et al.* 2001*b*). We also used a second analysis approach where we quantified the area occupied by PC^+ vesicles in a cluster by creating a binary image using a threshold pixel value set to discriminate between the vesicle membrane and lumen of PC^- vesicles. The number of pixels below threshold (electron-dense) was then divided by the total number of pixels occupied by the cluster to generate a fractional measure of electron-dense signal. For 3D reconstruction we aligned digital images of serial sections from our synapse of interest using multiple membrane and organelle landmarks. Models were built in Reconstruct (Synapse Web, Kristen M. Harris, http://synapses.clm.utexas.edu/) and rendered using Blender (Blender foundation, Amsterdam, The Netherlands).

Results

A variable fraction of recycling vesicles in hippocampal synapses

We looked at the basal variability of recycling vesicle fractions in our cultures using two approaches. First, neurons were transfected with synaptophysinI-mCherry (sypI-mCherry, Fig. 1*A*) to mark the total vesicle pool
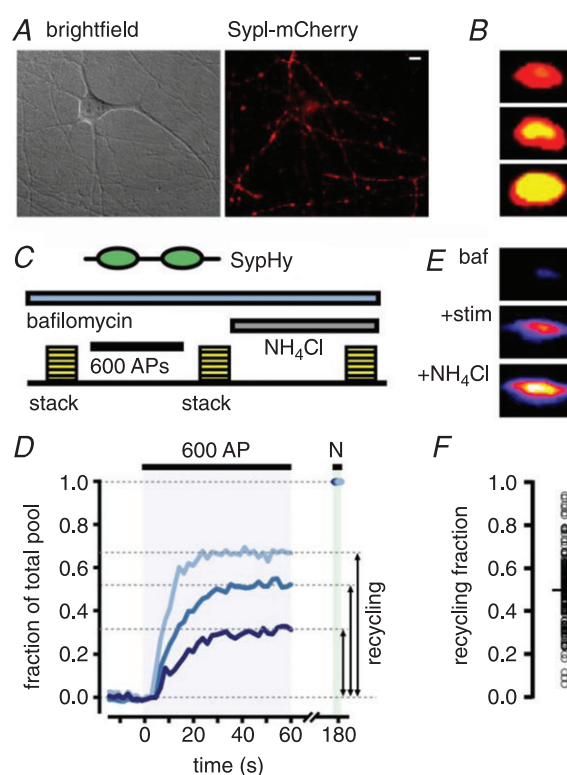
Figure 1. Measuring the variable vesicle recycling pool fraction in populations of hippocampal synapses
A, sample region in DIC (left) and with sypI-mCherry fluorescence showing typical target synapses (right). *B*, synapses loaded with FM1-43 (10 Hz, 600 APs) and expressing sypI-mCherry illustrating variability in the recycling vesicle subset of the total vesicle pool. Yellow represents overlap between green FM1-43 and red sypI-mCherry signal. *C*, schematic diagram of experiment for quantifying the recycling vesicle fraction using sypHy (see text). *D*, three sample traces of sypHy fluorescence showing a range of recycling vesicle fractions. *E*, sample images from a single synapse showing the three steps in the protocol for determining the recycling fraction. *F*, summary plot showing recycling fractions for 151 synapses from 3 experiments based on sypHy measurements. Black circle and horizontal line indicate mean fraction (0.49, SD: 0.16). Scale bar, $5\,\mu\text{m}$.

and stimulated in the presence of the activity-dependent styryl dye FM1-43 (Betz & Bewick, 1992; Ryan *et al.* 1993) to label the recycling pool. Dual imaging experiments revealed a variable ratio of these fluorescence markers in different synapses (Fig. 1*B*) indicating heterogeneity in the recycling vesicle pool subset of the total pool within synaptic populations. Second, to directly quantify this, we used the genetically encoded optical reporter sypHy, a fusion construct of the vesicle protein synaptophysin and pH-sensitive pHluorin, which reports vesicle exocytosis with a rise in fluorescence (Granseth *et al.* 2006). Experiments were carried out in the presence of bafilomycin (1 μM), a vATPase blocker which prevents the requenching of sypHy fluorescence by inhibiting vesicle reacidification ('alkaline trapping', Fig. 1*C*; Sankaranarayanan & Ryan, 2001). SypHy-expressing synapses were stimulated to activate the recycling pool and subsequently washed in NH$_4$Cl (50 mM) to de-quench all fluorescence signal and give a measure of total vesicle content (Fig. 1*C*–*E*). The relative difference between the stimulation-evoked and NH$_4$Cl-evoked signal is a quantitative estimate of the recycling fraction of the total vesicle pool at each synapse (Fig. 1*D* and *E*; Fernandez-Alfonso & Ryan, 2008; Kim & Ryan, 2010). These experiments revealed that

releasable fractions in a synaptic population were broadly distributed with a mean value of 0.49 (SD: 0.16, 151 synapses from 3 experiments; Fig. 1*F*). Taken together, our results demonstrate that the recycling vesicle fraction is approximately half the total pool size, but that this fraction is highly variable between individual synapses (see also Harata *et al.* 2001*b*; Li *et al.* 2005; Micheva & Smith, 2005; Fernandez-Alfonso & Ryan, 2008; Fredj & Burrone, 2009; Branco *et al.* 2010; Kim & Ryan, 2010; Welzel *et al.* 2011).

Tetanus-induced increase in recycling synaptic vesicle fraction

One possible explanation for the variable fraction of recycling vesicles observed in basal conditions is that this parameter is under regulatory control and can be locally modulated with appropriate conditions. We reasoned that activity-dependent plasticity might be one possible modulator. To test this hypothesis, we subjected neurons to a plasticity protocol in which cells received spaced tetanic stimulation (Ninan *et al.* 2006) in the presence or absence of a selective NMDAR receptor blocker (AP5). Recycling pool sizes were monitored using FM-dyes, by collecting z-stacks of labelled synapses before and 20 min after the tetanus (Fig. 2*A*). To alleviate concerns
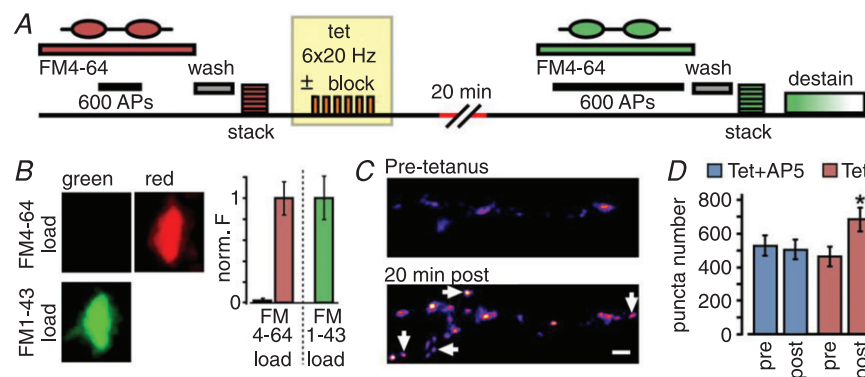
Figure 2. NMDA receptor-dependent plasticity protocol brings about specific changes in properties of recycling pools at individual synapses
A, schematic diagram of plasticity protocol. Synaptic recycling pools were maximally loaded with FM4-64 using field stimulation and an image stack was obtained. Cultures were then given spaced tetanic stimulation (6 × 100 APs, 20 Hz) in the presence or absence of AP-5 and returned to normal recording solution for 20–40 min. Neurons were then reloaded using FM1-43 and a second image stack collected. Stimulation to evoke dye-destaining was performed at the end of most experiments to check recycling competence. *B*, validation of two-dye FM-loading protocol for plasticity experiments. Left, demonstration of the absence of fluorescence bleed-through in our imaging system. An FM4-64 load at a presynaptic terminal is clearly visible in the red imaging channel (top right) but there is no evidence of bleed-through into the green channel (top left), as expected. Therefore, a second load with FM1-43 appearing in the green channel (bottom left) will not include a contribution of residual red fluorescence from the first load. In this way, independent and uncontaminated readouts for recycling pools can be collected in each FM-loading step. Right, bar graph quantifying the absence of fluorescence bleed-through. FM4-64 load (left bars) gave a negligible signal in the green channel (left-most bar, 0.02 ± 0.02) when expressed as a fraction of green fluorescence after FM1-43 loading (right bar). *C*, sample FM-dye image panels for a synaptic region pre- and post-tetanus, showing addition of new fluorescent puncta (arrows) and increase in fluorescence intensity (see text). *D*, summary of total number of puncta identified pre- and post-tetanus (tetanus+AP5, pre: 531 ± 61, post: 509 ± 59, paired *t* test, *P* = 0.76, *n* = 4 experiments; tetanus alone, pre: 467 ± 58, post: 685 ± 70, *P* < 0.05, *n* = 11 experiments).

that post-tetanic dye signal would be contaminated by residual signal from the first load, we used different FM-dyes (FM4-64 and FM1-43, respectively) for the pre- and post-labelling. The validation of this approach is summarized in Fig. 2*B*. To ensure unbiased analysis, FM-dye labelled synapses were automatically selected using a custom-written algorithm based on edge detection (see Methods). Consistent with previous findings using a variety of plasticity-induction protocols that report changes in key presynaptic parameters (Malgaroli *et al.* 1995; Ryan *et al.* 1996; Ma *et al.* 1999; Antonova *et al.* 2001; Micheva & Smith, 2005; Wang *et al.* 2005; Ninan *et al.* 2006; Tyler *et al.* 2006; Antonova *et al.* 2009) we observed significant increases in puncta number (Fig. 2*C* and *D*) and mean fluorescence intensity for the unblocked tetanus condition *versus* control (tetanus+AP5, 1.00 ± 0.02, tetanus alone, 1.40 ± 0.21, $P < 0.05$, Mann–Whitney, $n = 4$ and 11 experiments) suggesting that NMDAR activation-dependent changes had taken place.

Next, to specifically investigate potential changes in recycling pool fractions, we used our analysis software to carry out a pair analysis restricted to synaptic puncta that were unequivocally present in both images (Fig. 3*A*). In this way, we could examine plasticity-dependent changes in recycling vesicle properties occurring only at pre-existing terminals, rather than those arising as a consequence of *de novo* synthesis, synaptic splitting (Ma *et al.* 1999; Antonova *et al.* 2001; Ninan *et al.* 2006) or presynaptic unsilencing (Moulder *et al.* 2008; Cousin & Evans, 2011). Using this approach we found that synapses subjected to tetanic stimulation without NMDA receptor block showed significant relative increases in size (Fig. 3*B*–*D*) but also mean intensity (Fig. 3*B*–*D*, statistical analysis in figure legends) compared to conditions using AP5. As expected, activation of NMDA receptors was sufficient to induce potentiation: blockade of AMPA receptors alone did not prevent tetanus-induced synaptic changes. Taken together these results show that functional
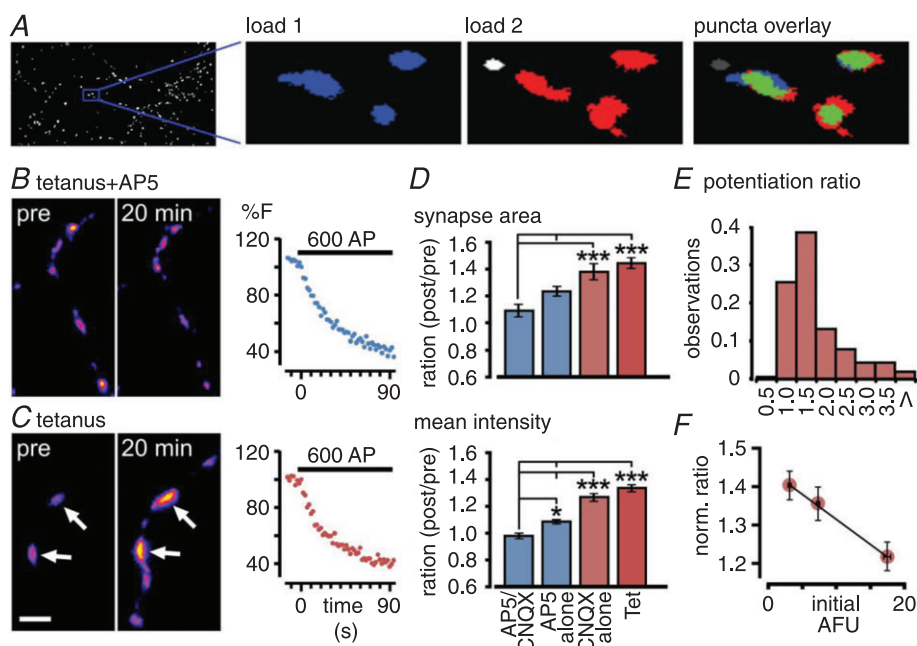
Figure 3. Plasticity induction increases the vesicle recycling fraction at individual stable synapses
A, sample images from analysis software demonstrate how fluorescence images (left panel) are used to generate masks (middle panels) which are overlaid to identify stable terminals which are present in both loads. *B* and *C*, sample pre/post image pairs for tetanus+AP5 (*B*) and tetanus alone conditions (*C*). Arrows indicate synapses with increased fluorescence. Right, FM1-43 destaining curves at the end of the experiment show recycling competence. *D*, summary of changes in area (top) and mean intensity (bottom) FM-dye fluorescence after 20 min for tetanus+CNQX+AP5, tetanus+AP5, tetanus+CNQX and tetanus alone conditions. Bar graphs show ratios (post/pre) for each condition. Area: ANOVA, $P < 0.0001$; Tukey's test: Tet *vs.* Tet+CNQX, $P > 0.05$ ($n = 1058$ from 11 experiments and $n = 426$ from 3 experiments, respectively); Tet *vs.* Tet+AP5, $P < 0.001$ ($n = 787$ from 4 experiments); Tet *vs.* Tet+CNQX+AP5, $P < 0.001$ ($n = 433$ from 7 experiments). Mean fluorescence: ANOVA, $P < 0.0001$; Tukey's test: Tet *vs.* Tet+CNQX, $P > 0.05$ ($n = 1058$ from 11 experiments and $n = 426$ from 3 experiments, respectively); Tet *vs.* Tet+AP5, $P < 0.001$ ($n = 787$ from 4 experiments); Tet *vs.* Tet+CNQX+AP5, $P < 0.001$ ($n = 433$ from 7 experiments). *$P < 0.05$, **$P < 0.01$, ***$P < 0.001$. *E*, frequency histogram for tetanus alone showing the distribution of potentiation ratios across all synapses (1057 synapses from 11 experiments). *F*, plot of relationship between initial integrated intensity of synapses and post/pre mean intensity ratio. Line is a linear fit to data points.

recycling pools associated with persistent synapses can readily increase following tetanus and, in particular, the density of recycling vesicles per unit area or fractional recycling pool size is elevated. Notably, only a subset of synapses were potentiated (Fig. 3*E*). We reasoned that one possible variable related to this capability might be the initial recycling pool size. To test this, we plotted the initial integrated fluorescence at a synapse against its fractional change in mean intensity following tetanus (Fig. 3*F*). We found an inverse relationship between these variables implying that small synapses show larger relative changes in their recycling pool fraction compared to larger synapses, consistent with previous reports suggesting that small synapses are more susceptible to plastic changes (Ryan *et al.* 1993; Malgaroli *et al.* 1995).

Our analysis strongly implies that the relative proportion of functional vesicles at a synaptic terminal may be increased under potentiating conditions. To test this directly we next carried out plasticity experiments on neurons expressing sypHy (Granseth *et al.* 2006), using the alkaline trapping method outlined above. In this case we could make direct measurements of the recycling fraction of the total pool at each synapse following our potentiation protocol. In tetanus+AP5 controls, we measured a mean recycling fraction of 0.44 (SD: 0.1852, $n = 55$ from 3 experiments) but unblocked tetanus resulted in a significant increase in the mean fraction of recycling vesicles (0.66, SD: 0.20, $n = 141$ synapses from 4 experiments, $P < 0.01$, Student's *t* test; Fig. 4*C*). We also tested a stronger tetanic stimulation protocol (6×40 Hz) but notably, this resulted in a similar level of potentiation (0.67, SD: 0.03) implying that stronger stimulation does

not recruit additional vesicles to the functional pool. Taken together these results show that the functional recycling pool at persistent synapses readily increases following tetanus and, specifically, that the fractional recycling pool size is elevated at the expense of the resting pool.

Ultrastructural analysis of potentiated synapses

We next combined FM-dye experiments with correlative ultrastructural analysis to provide direct ultrastructural evidence for changes in functional vesicle pool fractions. FM1-43FX fluorescence image z-stacks from tetanus-blocked and tetanus-unblocked cultures were collected then fixed, and subsequently target regions were photoconverted in the presence of diaminobenzidine to generate an electron-dense product associated with FM-dye staining (Harata *et al.* 2001*b*; Schikorski & Stevens, 2001; Rizzoli & Betz, 2004; Darcy *et al.* 2006*a,b*) (Fig. 5*A*). Embedded samples were serially sectioned and viewed in EM and fluorescence maps were overlaid on electron micrographs to locate target synaptic terminals (Fig. 5*B* and *C*). To provide an unbiased sampling of our synaptic population at EM level, we generated fluorescence intensity distribution curves for experimental and control synapses and targeted all puncta in the top 40% of the distribution. Of these we could unequivocally correlate a subset in our EM samples (tetanus: 28 synapses, mean section number: 4.39; tetanus + block: 37 synapses, mean section number: 4.13).

In both groups, vesicle clusters containing photo-converted (PC^+) and non-photoconverted (PC^-) vesicles were readily observed (Fig. 5*A*). We counted the numbers
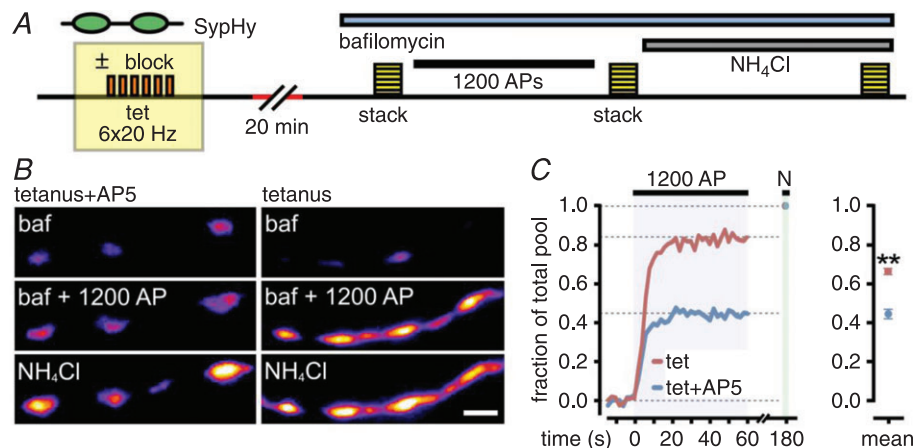
Figure 4. Direct measurement of plasticity-induced changes in recycling vesicle fraction using sypHy and alkaline trapping
A, schematic diagram of experiment (see results). *B*, sample experimental images for tetanus+AP5 and tetanus alone conditions. Image panels are pre-stimulation (bafilomycin, 'baf'), after 1200 APs, and after wash with 50 mM NH$_4$Cl. *C*, left, sample traces showing different recycling fractions for tetanus (red) and tetanus+AP5 (blue) synapse. N: NH$_4$Cl treatment. Right, summary of recycling vesicle fractions. **$P < 0.01$. All plots show mean ± SEM. Scale bars, 2 μm.

of PC$^+$ and PC$^-$ vesicles to provide a score of the recycling vesicle fraction at each synapse. Our quantification revealed that while recycling fractions were variable in both conditions, the tetanus group had significantly higher fractions and a narrower distribution when compared to control (tetanus: 0.65 ± 0.02, CV $= 0.13$, from 28 synapses; tetanus+block: 0.52 ± 0.02, CV $= 0.23$, from 37 synapses; $P < 0.01$, Student's *t* test, Fig. 5*D–G*). As an independent confirmation of our findings, we also used a separate quantification approach based on thresholding (see Methods) which revealed the same difference between experimental and control synapses (tetanus: 0.81 ± 0.01, from 20 synapses; tetanus+block: 0.67 ± 0.02, from 20 synapses; $P < 0.01$, Student's *t* test; note: numbers are not directly equivalent to fractions given above since all vesicles include electron-dense membrane). The elevated recycling fraction in the unblocked tetanus group was readily visible at the level of individual synapses (Fig. 5*C–G*). Frequency histogram plots revealed that the distribution of recycling fractions was shifted to the right in the unblocked tetanus group but, notably, did not exceed 0.8 (Fig. 5*H*) suggesting a possible ceiling for the recruitment of resting pool vesicles under our treatment conditions.

Increase in release probability accompanies tetanus-induced potentiation

We next investigated the direct effects of the plasticity protocol on synaptic function by estimating release probability (p_r; Branco & Staras, 2009) at individual terminals. Cultures were subjected to tetanus or tetanus+AP5 and subsequently FM-dye-loaded (Fig. 6*A*). To measure p_r we imaged activity-evoked dye-loss at 1 Hz stimulation frequency for 600 APs (Fig. 6*A* and *B*), where the rate of fluorescence decay is proportional to release probability (Zakharenko *et al.* 2001; Branco *et al.* 2010) (see Methods). In tetanus + AP5 conditions, the mean

Figure 5. Increases in recycling vesicle pool fractions seen at ultrastructural level after FM-dye photoconversion
A, image and plot showing two clearly distinct vesicle classes, photoconverted (PC+, with dark lumen) and non-photoconverted (PC− with empty lumen). Plot shows the inverse of normalized intensity for line profiles of 8 PC$^+$ and 8 PC$^-$ vesicles from 2 synapses. *B*, illustration of correlative fluorescence-EM method. Synaptic puncta were identified in fluorescence images and overlaid on low power electron micrographs (left panel with fluorescence, right panel as outline). Inset, detail of a target terminal from tetanus group. *C*, low power electron micrograph from tetanus experiment,

illustrating a cluster of synapses along an axon (white boxes) exhibiting high recycling fractions. *D*, left three panels, sample images of synapses from tetanus conditions. Right panel, example of a synapse from the tetanus group whose fluorescence was not in the top 40%. The low PC$^+$ count in this synapse illustrates that the high recycling fractions observed in the experimental synaptic population are not explained by a non-specific effect such as excessive photoconversion. *E*, sample images from Tet+block synapses. *F*, 3D reconstruction of synapse from tetanus alone made from nine consecutive serial sections. The vesicle fraction for this synapse is 0.68, equivalent to the average recycling fraction seen in potentiated synapses. *G*, summary plot of recycling fraction for tetanus+block and tetanus alone. Dark circles and horizontal lines indicate mean fraction for each group. **$P < 0.01$. *H*, recycling pool fraction frequency histogram for both conditions from EM data (tetanus+block: 37 synapses, tetanus: 28 synapses).

destaining time constant (τ) was 246 ± 9 s and p_r showed a broad and skewed distribution (mean: 0.38 ± 0.02, 116 synapses from 3 experiments, Fig. 6C and D), consistent with previous findings (Murthy *et al.* 1997; Slutsky *et al.* 2004; Branco *et al.* 2008). By contrast, in unblocked terminals, the mean destaining rates were significantly faster (τ: 207 ± 10 s, $P < 0.01$, Student's *t* test, Fig. 6B and C) and the distribution of p_r was gaussian and shifted to higher values (mean: 0.53 ± 0.02, 82 synapses from 3 experiments; $P < 0.01$, Student's *t* test, Fig. 6D). Our findings suggest that tetanic stimulation mediating specific changes in vesicle recycling pools is also associated with increases in a key determinant of synaptic strength.

Changes in recycling fractions are sensitive to NO synthase and calcineurin inhibitors

Recent work has implicated cyclin-dependent kinase 5 and calcineurin in setting the relative recycling and resting pool sizes associated with a form of homeostatic scaling (Kim & Ryan, 2010), where calcineurin activity promotes increases in the recycling fraction. Reasoning that our potentiation might utilize the same mechanism, we tested the effect of the calcineurin blocker FK506 applied during the tetanus. Our findings demonstrated an effective abolishment of the increase in FM-dye signal observed in unblocked synapses (Fig. 7A, mean intensity Tet, 1.22 ± 0.05, 180 synapses from 2 experiments; Tet+FK506, 0.82 ± 0.03, 125 synapses from 4 experiments, $P < 0.01$, Student's *t* test).

The dependence of potentiation on NMDAR activation hints at the possible involvement of a retrograde message to permit presynaptic changes to take place. A likely candidate is NO, previously shown to participate in pre-synaptic plasticity (Wang *et al.* 2005) and we tested its role here by inhibiting NO synthase with N^{ω}-nitro-L-arginine (L-NA) during tetanus. Our findings showed that the tetanus-induced increase in the recycling fraction was blocked (Fig. 7B) suggesting that NO signalling contributes to presynaptic pool reorganization. A number of studies have established that synaptic vesicles are highly laterally mobile along axons (Krueger *et al.* 2003; Darcy *et al.* 2006a; Chen *et al.* 2008; Westphal *et al.* 2008; Staras *et al.* 2010; Fisher-Lavie *et al.* 2011; Herzog *et al.* 2011; Ratnayaka *et al.* 2011) and we reasoned that a component of the potentiation process might be due to the regulated recruitment of vesicles arising from outside the presynaptic terminal (Darcy *et al.* 2006a; Staras, 2007; Staras & Branco, 2010). To test this, we incubated neurons with jasplakinolide, an inhibitor of actin turnover, which effectively impairs lateral vesicle traffic (Fig. 7C; Darcy *et al.* 2006a). Notably, its impact on potentiation was marginal (Fig. 7B) suggesting that the import of extrasynaptic vesicles is not critical to support

the expansion of the recycling pool observed in this form of plasticity.

Discussion

We demonstrate here that a form of NMDAR-dependent potentiation can modulate the balance of vesicle pools at synaptic terminals, increasing the size of the functional recycling pool as a fraction of the total pool, and being associated with an increase in synaptic release probability. We propose that this is achieved by direct recruitment of vesicles from the resting pool, offering a rapid mechanism for adjusting synaptic performance at individual terminals to support a form of Hebbian potentiation.

The existence of a variable recycling vesicle pool fraction at hippocampal terminals is well established (Harata *et al.* 2001a,b; Li *et al.* 2005; Micheva & Smith, 2005; Fernandez-Alfonso & Ryan, 2008; Fredj & Burrone, 2009; Branco *et al.* 2010; Kim & Ryan, 2010; Welzel *et al.* 2011) and potential roles for the residual
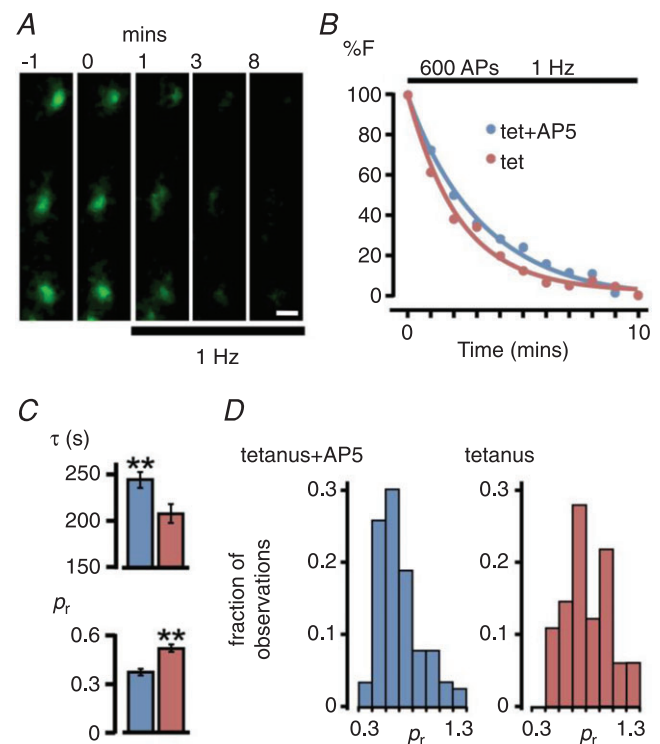
Figure 6. Plasticity induction mediates an increase in synaptic release probability
A, panels illustrating FM1-43 destaining during 1 Hz stimulation indicated by bar. Each image is a maximum intensity projection from a z-stack (5 planes). *B*, sample destaining curves normalized to total dye loss for synapses from tetanus+AP5 and tetanus groups for 1 Hz stimulation. *C*, summary bar graphs of mean destaining timecourse (τ) and estimated p_r for Tet+AP5 (blue) and Tet (red). Plots show means $\pm$ SEM; **$P < 0.01$. *D*, release probability frequency histogram for both conditions. Scale bar, 1 μm.

resting pool fraction have been extensively debated. Recent evidence suggests that one possible function of resting vesicles is as participants in spontaneous transmission (Sara *et al.* 2005; Fredj & Burrone, 2009) but this notion remains controversial (Groemer & Klingauf, 2007; Hua *et al.* 2010; Wilhelm *et al.* 2010). Another possibility (Fernandez-Alfonso & Ryan, 2008; Branco *et al.* 2010; Kim & Ryan, 2010) is that the resting pool fraction represents an available vesicle reserve that can be accessed for recruitment of vesicles to functional recycling pools as a possible mechanism for adjusting synaptic performance. Indeed, homeostatic responses to chronic synaptic silencing include long-term increases in recycling vesicle pools (Murthy *et al.* 2001; Thiagarajan *et al.* 2005). Recently, elegant work has provided a molecular mechanism for this type of homeostatic plasticity, implicating cyclin-dependent kinase 5 and calcineurin in setting the balance between recycling and resting pool fractions at presynaptic terminals (Kim & Ryan, 2010). However, while Hebbian forms of synaptic potentiation have been associated with changes in vesicle pool properties such as increases in the number of synaptic puncta (Ninan & Arancio, 2004; Ninan *et al.* 2006) and their fluorescence intensity (Ryan *et al.* 1996; Micheva & Smith, 2005; Ninan *et al.* 2006), as well as increases in vesicle release and turnover (Ryan *et al.* 1996; Zakharenko *et al.* 2001; Ninan *et al.* 2006; Tyler *et al.* 2006), the specific impact of potentiation on the balance between recycling and resting pools has not been established.

In the present study we have used three separate measures of the functional vesicle fraction to directly show that NMDAR-dependent synaptic potentiation can enhance the recycling pool at the expense of the resting pool. Our evidence suggests that potentiation does not specifically depend on extrasynaptic vesicle recruitment, indicating that changes in the functionality of existing vesicles residing stably at terminals are sufficient to account for this change. Taken together, these findings suggest a model where resting vesicles are specifically 'convertible' to recycling vesicles in response to particular levels and patterns of synaptic activity. Our results implicate calcineurin in this process, adding further weight to the emerging idea that this is a key substrate for setting pool sizes (Kumashiro *et al.* 2005; Kim & Ryan, 2010). We show that the potentiation mechanism identified here is sensitive to blockers of NMDARs and NO synthase. This suggests that the pathway of plasticity induction involves postsynaptic activation and retrograde signalling, consistent with a previous example of presynaptic plasticity reported in hippocampal neurons (Wang *et al.* 2005). One interesting aspect of our findings is that the magnitude of potentiation was not uniform across the synapse population. We observed that the capability for potentiation was highest in synapses with lower initial fluorescence intensity, indicating an inverse correlation between recycling pool size and this type of plastic change. A similar relationship between size and the capacity to undergo synaptic strengthening also has been reported by others both presynaptically (Ryan *et al.* 1993; Malgaroli *et al.* 1995) and postsynaptically (Bi & Poo, 1998). In our ultrastructural data, we always observed a subset of vesicles in potentiated synapses that
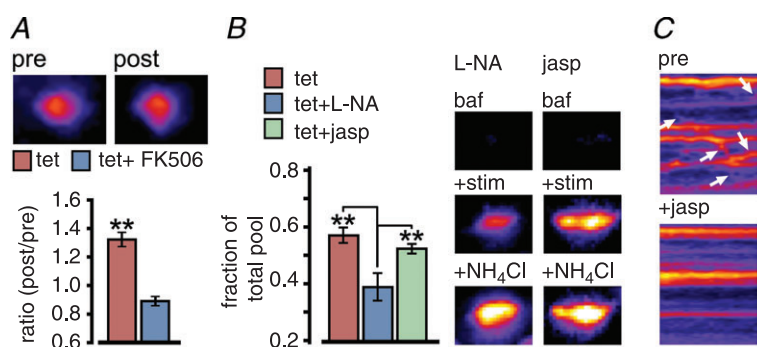
Figure 7. Potentiation is sensitive to calcineurin and NO synthase inhibitors but does not require actin polymerization

A, FM-dye loading protocol (see Fig. 2) used to test the influence of the calcineurin blocker FK506 on potentiation. Bar graph shows ratios (post/pre) for tetanus and tetanus+FK506. Inset (top) shows pre and post FM-dye fluorescence for a synapse treated with FK506. *B*, SypHy protocol (see Fig. 4) to test the effect of the NO synthase blocker L-NA and the actin inhibitor jasplakinolide on potentiation. Left, bar graph summarizing recycling fractions for tetanus, tetanus+L-NA and tetanus+jasplakinolide (Jasp). ANOVA, $P < 0.0001$; Tukey's: Tet *vs.* Tet+L-NA, $P < 0.001$, Tet *vs.* Tet+Jasp, $P > 0.05$, Tet+Jasp *vs.* Tet+L-NA, $P < 0.001$, $n = 57$ synapses from 3 experiments, $n = 57$ synapses from 3 experiments, $n = 76$ synapses from 4 experiments, respectively). *$P < 0.05$, **$P < 0.01$, ***$P < 0.001$. Right, sample images of synapses illustrating recycling pool (+stim) and total pool (+NH$_4$Cl) after plasticity in L-NA and jasplakinolide. *C*, kymographs generated from an FM1-43-labelled axonal segment demonstrating inhibition of lateral vesicle movement (arrows) after jasplakinolide. Horizontal scale bar, 30 s; vertical bar, 2 μm.

were not electron-dense. This suggests that under our treatment conditions, some vesicles appeared not to be converted into recycling vesicles, raising the possibility of a non-recruitable vesicle subpool. Nonetheless, a much broader analysis using a range of different potentiating treatment paradigms would be necessary to determine if such a non-functional pool was a persistently conserved feature of synaptic terminals.

Our findings support the emerging view that interactions between distinct vesicle pools are a major control mechanism for adjusting synaptic efficacy (Branco *et al.* 2010; Kim & Ryan, 2010). Similar reserve pools and their ability to undergo functional activation also have been reported in other systems such as *Drosophila* neuromuscular junction (Kuromi & Kidokoro, 2000; Akbergenova & Bykhovskaia, 2009). The idea that the resting pool is a recruitable vesicle reserve offers an explanation for why this substantial dormant pool is maintained at synapses, presumably at considerable energetic costs (Ikeda & Bekkers, 2009), and why its specific size is highly variable across synaptic populations. Resting and recycling vesicle pools are a defining feature of most synapses in the CNS and our findings suggest that rapid vesicle exchange between these two pools may represent a novel and widespread substrate for synaptic strength adjustments during Hebbian plasticity.

References

Akbergenova Y & Bykhovskaia M (2009). Stimulation-induced formation of the reserve pool of vesicles in *Drosophila* motor boutons. *J Neurophysiol* **101**, 2423–2433.

Antonova I, Arancio O, Trillat AC, Wang HG, Zablow L, Udo H, Kandel ER & Hawkins RD (2001). Rapid increase in clusters of presynaptic proteins at onset of long-lasting potentiation. *Science* **294**, 1547–1550.

Antonova I, Lu FM, Zablow L, Udo H & Hawkins RD (2009). Rapid and long-lasting increase in sites for synapse assembly during late-phase potentiation in rat hippocampal neurons. *PLoS One* **4**, e7690.

Betz WJ & Bewick GS (1992). Optical analysis of synaptic vesicle recycling at the frog neuromuscular junction. *Science* **255**, 200–203.

Bi GQ & Poo MM (1998). Synaptic modifications in cultured hippocampal neurons: dependence on spike timing, synaptic strength, and postsynaptic cell type. *J Neurosci* **18**, 10464–10472.

Branco T, Marra V & Staras K (2010). Examining size-strength relationships at hippocampal synapses using an ultrastructural measurement of synaptic release probability. *J Struct Biol* **172**, 203–210.

Branco T & Staras K (2009). The probability of neurotransmitter release: variability and feedback control at single synapses. *Nat Rev Neurosci* **10**, 373–383.

Branco T, Staras K, Darcy KJ & Goda Y (2008). Local dendritic activity sets release probability at hippocampal synapses. *Neuron* **59**, 475–485.

Chen X, Barg S & Almers W (2008). Release of the styryl dyes from single synaptic vesicles in hippocampal neurons. *J Neurosci* **28**, 1894–1903.

Cousin MA & Evans GJ (2011). Activation of silent and weak synapses by cAMP-dependent protein kinase in cultured cerebellar granule neurons. *J Physiol* **589**, 1943–1955.

Darcy KJ, Staras K, Collinson LM & Goda Y (2006*a*). Constitutive sharing of recycling synaptic vesicles between presynaptic boutons. *Nat Neurosci* **9**, 315–321.

Darcy KJ, Staras K, Collinson LM & Goda Y (2006*b*). An ultrastructural readout of fluorescence recovery after photobleaching using correlative light and electron microscopy. *Nat Protoc* **1**, 988–994.

Fernandez-Alfonso T & Ryan TA (2006). The efficiency of the synaptic vesicle cycle at central nervous system synapses. *Trends Cell Biol* **16**, 413–420.

Fernandez-Alfonso T & Ryan TA (2008). A heterogeneous 'resting' pool of synaptic vesicles that is dynamically interchanged across boutons in mammalian CNS synapses. *Brain Cell Biol.* **36**, 87–100.

Fisher-Lavie A, Zeidan A, Stern M, Garner CC & Ziv NE (2011). Use dependence of presynaptic tenacity. *J Neurosci* **31**, 16770–16780.

Fredj NB & Burrone J (2009). A resting pool of vesicles is responsible for spontaneous vesicle fusion at the synapse. *Nat Neurosci* **12**, 751–758.

Granseth B, Odermatt B, Royle SJ & Lagnado L (2006). Clathrin-mediated endocytosis is the dominant mechanism of vesicle retrieval at hippocampal synapses. *Neuron* **51**, 773–786.

Groemer TW & Klingauf J (2007). Synaptic vesicles recycle spontaneously and during activity belong to the same vesicle pool. *Nat Neurosci* **10**, 145–147.

Harata N, Pyle JL, Aravanis AM, Mozhayeva M, Kavalali ET & Tsien RW (2001*a*). Limited numbers of recycling vesicles in small CNS nerve terminals: implications for neural signaling and vesicular cycling. *Trends Neurosci* **24**, 637–643.

Harata N, Ryan TA, Smith SJ, Buchanan J & Tsien RW (2001*b*). Visualizing recycling synaptic vesicles in hippocampal neurons by FM 1-43 photoconversion. *Proc Natl Acad Sci U S A* **98**, 12748–12753.

Herzog E, Nadrigny F, Silm K, Biesemann C, Helling I, Bersot T, Steffens H, Schwartzmann R, Nagerl UV, El Mestikawy S, Rhee J, Kirchhoff F & Brose N (2011). In vivo imaging of intersynaptic vesicle exchange using VGLUT1 Venus knock-in mice. *J Neurosci* **31**, 15544–15559.

Hua Y, Sinha R, Martineau M, Kahms M & Klingauf J (2010). A common origin of synaptic vesicles undergoing evoked and spontaneous fusion. *Nat Neurosci* **13**, 1451–1453.

Ikeda K & Bekkers JM (2009). Counting the number of releasable synaptic vesicles in a presynaptic terminal. *Proc Natl Acad Sci U S A* **106**, 2945–2950.

Kim SH & Ryan TA (2010). CDK5 serves as a major control point in neurotransmitter release. *Neuron* **67**, 797–809.

Krueger SR, Kolar A & Fitzsimonds RM (2003). The presynaptic release apparatus is functional in the absence of dendritic contact and highly mobile within isolated axons. *Neuron* **40**, 945–957.

Kumashiro S, Lu YF, Tomizawa K, Matsushita M, Wei FY & Matsui H (2005). Regulation of synaptic vesicle recycling by calcineurin in different vesicle pools. *Neurosci Res* **51**, 435–443.

Kuromi H & Kidokoro Y (2000). Tetanic stimulation recruits vesicles from reserve pool via a cAMP-mediated process in *Drosophila* synapses. *Neuron* **27**, 133–143.

Li Z, Burrone J, Tyler WJ, Hartman KN, Albeanu DF & Murthy VN (2005). Synaptic vesicle recycling studied in transgenic mice expressing synaptopHluorin. *Proc Natl Acad Sci U S A* **102**, 6131–6136.

Ma L, Zablow L, Kandel ER & Siegelbaum SA (1999). Cyclic AMP induces functional presynaptic boutons in hippocampal CA3–CA1 neuronal cultures. *Nat Neurosci* **2**, 24–30.

Malgaroli A, Ting AE, Wendland B, Bergamaschi A, Villa A, Tsien RW & Scheller RH (1995). Presynaptic component of long-term potentiation visualized at individual hippocampal synapses. *Science* **268**, 1624–1628.

Micheva KD & Smith SJ (2005). Strong effects of subphysiological temperature on the function and plasticity of mammalian presynaptic terminals. *J Neurosci* **25**, 7481–7488.

Moulder KL, Jiang X, Chang C, Taylor AA, Benz AM, Conti AC, Muglia LJ & Mennerick S (2008). A specific role for Ca^{2+}-dependent adenylyl cyclases in recovery from adaptive presynaptic silencing. *J Neurosci* **28**, 5159–5168.

Murthy VN, Schikorski T, Stevens CF & Zhu Y (2001). Inactivity produces increases in neurotransmitter release and synapse size. *Neuron* **32**, 673–682.

Murthy VN, Sejnowski TJ & Stevens CF (1997). Heterogeneous release properties of visualized individual hippocampal synapses. *Neuron* **18**, 599–612.

Ninan I & Arancio O (2004). Presynaptic CaMKII is necessary for synaptic plasticity in cultured hippocampal neurons. *Neuron* **42**, 129–141.

Ninan I, Liu S, Rabinowitz D & Arancio O (2006). Early presynaptic changes during plasticity in cultured hippocampal neurons. *EMBO J* **25**, 4361–4371.

Ostroff LE, Cain CK, Jindal N, Dar N & Ledoux JE (2011). Stability of presynaptic vesicle pools and changes in synapse morphology in the amygdala following fear learning in adult rats. *J Comp Neurol* **520**, 295–314.

Pechstein A & Shupliakov O (2010). Taking a back seat: synaptic vesicle clustering in presynaptic terminals. *Front Synaptic Neurosci* **2**, 143.

Ratnayaka A, Marra V, Branco T & Staras K (2011). Extrasynaptic vesicle recycling in mature hippocampal neurons. *Nat Comms* **2**, 531.

Rizzoli SO & Betz WJ (2004). The structural organization of the readily releasable pool of synaptic vesicles. *Science* **303**, 2037–2039.

Rizzoli SO & Betz WJ (2005). Synaptic vesicle pools. *Nat Rev Neurosci* **6**, 57–69.

Ryan TA, Reuter H & Smith SJ (1997). Optical detection of a quantal presynaptic membrane turnover. *Nature* **388**, 478–482.

Ryan TA, Reuter H, Wendland B, Schweizer FE, Tsien RW & Smith SJ (1993). The kinetics of synaptic vesicle recycling measured at single presynaptic boutons. *Neuron* **11**, 713–724.

Ryan TA & Smith SJ (1995). Vesicle pool mobilization during action potential firing at hippocampal synapses. *Neuron* **14**, 983–989.

Ryan TA, Ziv NE & Smith SJ (1996). Potentiation of evoked vesicle turnover at individually resolved synaptic boutons. *Neuron* **17**, 125–134.

Sankaranarayanan S & Ryan TA (2001). Calcium accelerates endocytosis of vSNAREs at hippocampal synapses. *Nat Neurosci* **4**, 129–136.

Sara Y, Virmani T, Deak F, Liu X & Kavalali ET (2005). An isolated pool of vesicles recycles at rest and drives spontaneous neurotransmission. *Neuron* **45**, 563–573.

Schikorski T & Stevens CF (2001). Morphological correlates of functionally defined synaptic vesicle populations. *Nat Neurosci* **4**, 391–395.

Schweizer FE & Ryan TA (2006). The synaptic vesicle: cycle of exocytosis and endocytosis. *Curr Opin Neurobiol* **16**, 298–304.

Slutsky I, Sadeghpour S, Li B & Liu G (2004). Enhancement of synaptic plasticity through chronically reduced Ca^{2+} flux during uncorrelated activity. *Neuron* **44**, 835–849.

Staras K (2007). Share and share alike: trading of presynaptic elements between central synapses. *Trends Neurosci* **30**, 292–298.

Staras K & Branco T (2010). Sharing vesicles between central presynaptic terminals: implications for synaptic function. *Front Synaptic Neurosci* **2**, 20.

Staras K, Branco T, Burden JJ, Pozo K, Darcy KJ, Marra V, Ratnayaka A & Goda Y (2010). A vesicle superpool spans multiple presynaptic terminals in hippocampal neurons. *Neuron* **66**, 37–44.

Sudhof TC (2004). The synaptic vesicle cycle. *Annu Rev Neurosci* **27**, 509–547.

Thiagarajan TC, Lindskog M & Tsien RW (2005). Adaptation to synaptic inactivity in hippocampal neurons. *Neuron* **47**, 725–737.

Tyler WJ, Zhang XL, Hartman K, Winterer J, Muller W, Stanton PK & Pozzo-Miller L (2006). BDNF increases release probability and the size of a rapidly recycling vesicle pool within rat hippocampal excitatory synapses. *J Physiol* **574**, 787–803.

Wang HG, Lu FM, Jin I, Udo H, Kandel ER, de Vente J, Walter U, Lohmann SM, Hawkins RD & Antonova I (2005). Presynaptic and postsynaptic roles of NO, cGK and RhoA in long-lasting potentiation and aggregation of synaptic proteins. *Neuron* **45**, 389–403.

Welzel O, Henkel AW, Stroebel AM, Jung J, Tischbirek CH, Ebert K, Kornhuber J, Rizzoli SO & Groemer TW (2011). Systematic heterogeneity of fractional vesicle pool sizes and release rates of hippocampal synapses. *Biophys J* **100**, 593–601.

Westphal V, Rizzoli SO, Lauterbach MA, Kamin D, Jahn R & Hell SW (2008). Video-rate far-field optical nanoscopy dissects synaptic vesicle movement. *Science* **320**, 246–249.

Wilhelm BG, Groemer TW & Rizzoli SO (2010). The same synaptic vesicles drive active and spontaneous release. *Nat Neurosci* **13**, 1454–1456.

Zakharenko SS, Zablow L & Siegelbaum SA (2001). Visualization of changes in presynaptic function during long-term synaptic plasticity. *Nat Neurosci* **4**, 711–717.

Author contributions

K.S. conceived the study and K.S., A.R. and V.M. designed the experiments. K.S., A.R., V.M., T.B., D.B. and J.J.B. collected, analysed and interpreted the data. K.S. initially drafted the manuscript and A.R., V.M, T.B and D.B. revised it. All authors approved the final version of the manuscript.